Proton Halo of ^{8}B Disclosed by Its Giant Quadrupole Moment

T. Minamisono,[1] T. Ohtsubo,[1] I. Minami,[1] S. Fukuda,[1] A. Kitagawa,[1,a] M. Fukuda,[1] K. Matsuta,[1] Y. Nojiri,[1] S. Takeda,[2] H. Sagawa,[3] and H. Kitagawa[4]

[1]*Department of Physics, and Laboratory of Nuclear Studies, Faculty of Science, Osaka University, 1-1 Machikaneyama, Toyonaka, Osaka 560, Japan*

[2]*Department of Chemistry, Faculty of Science, Osaka University, 1-1 Machikaneyama, Toyonaka, Osaka 560, Japan*

[3]*Department of Physics, Faculty of Science, The University of Tokyo, 7-3-1 Hongou 7-3-1, Bunkyo, Tokyo 113, Japan*

[4]*Research Center for Nuclear Physics, Osaka University, 10-1 Mihogaoka, Ibaraki, Osaka 567, Japan*

(Received 29 May 1992)

The quadrupole moment of the ^{8}B ($I^{\pi}=2^{+}$, $T_{1/2}=769$ msec) nucleus was measured as $|Q(^{8}\mathrm{B})|=68.3\pm2.1$ mb by use of modified β-NMR. This value is twice as large as the prediction of the Cohen-Kurath shell model. It is found by subtracting the contribution of deeply bound neutrons that the protons in ^{8}B carry more than 90% of the observed moment. The anomalous value is accounted for fairly well by the proton halo due to the loosely bound valence configuration. This is the first experimental evidence for the existence of a proton halo covering a neutron core.

PACS numbers: 21.10.Ky, 21.10.Ft, 27.20.+n

Nuclear properties that depend upon isospin will be enhanced and clearly observed in high isospin states, i.e., in those nuclei located near the proton and neutron drip lines in the mass chart. One of the peculiar observables of those nuclei is the radius of the nuclear matter distribution. For example, from the measurements of interaction cross sections by use of a high-energy nuclear beam of unstable neutron-rich ^{11}Li, a neutron halo covering the ^{9}Li core was found by Tanihata *et al.* [1]. Regarding the proton halo, however, no signals have been reported yet. It is quite natural to expect such a halo for protons because of the charge symmetry of the nuclear force. However, the Coulomb force among the protons besides the nuclear force may prevent the growth of the halo and push the proton inside the Coulomb barrier. As a result, the proton halo may be less pronounced than the neutron halo even if it is formed. From an experimental point of view, it is difficult to detect the thin halo by such cross-section measurements because the method is mainly designed to observe matter distributions, and therefore the effect due to the proton halo could be only a small fraction of the cross section. For an investigation of the proton halo, on the other hand, quadrupole moments are the most suitable probe, since they reflect dominantly the radial and angular distributions of the valence protons in the case of spherical nuclei. Of specific interest is the quadrupole moment of the ^{8}B ($I^{\pi}=2^{+}$, $T_{1/2}=769$ msec) nucleus because it is located near the proton drip line. It is expected that the proton distribution swells out radially in this nucleus because the separation energy of one proton is very small, 0.14 MeV, while, on the contrary, that of the neutron is large, 13 MeV. This means that the valence protons are very loosely bound at the shallow ridge of the nuclear potential, while the neutrons are very tightly bound.

β-NMR detections [2] are the most promising method to measure the quadrupole moments of ^{8}B since it is a short-lived β emitter. As is well known, however, the detection of the quadrupole effects in the β-NMR of such unstable nuclei with a nuclear lifetime of about 1 sec is usually very difficult, and time consuming, because of the complexity of the spectral shape and small NMR effect due to its higher spin ($I=2$ for ^{8}B), and because of the poor knowledge of the electric field gradients. Therefore, new techniques are required for an efficient and precise measurement of the quadrupole coupling constant of the unstable ^{8}B in some crystals. At the same time, remeasurements of the electric field gradients in the crystals are needed for the extraction of such precise values.

In this Letter we describe a precise measurement of the quadrupole moment $Q(^{8}\mathrm{B},2^{+})$ by use of a newly developed nuclear quadrupole resonance technique (NNQR), and also a precise measurement of the quadrupole moment $Q(^{8}\mathrm{Li},2^{+})$ of $^{8}\mathrm{Li}(2^{+})$ which is the mirror partner of ^{8}B. These precise values allow a detailed discussion on the proton distribution in the ^{8}B nucleus.

The experimental method and equipment used in the present measurements were essentially the same as in our previous works [3,4] on ^{12}B implanted in ZrB_2 and Mg metals. Major improvements are in the selection of implantation media for well-defined field gradients, and in the newly developed NNQR for efficient measurements of eqQ/h. In the standard technique of β-NMR [2], the ^{8}B nuclei were produced through a $^{6}\mathrm{Li}(^{3}\mathrm{He},n)^{8}\mathrm{B}$ reaction at the incident energy of 4.6 MeV. The beam-on production time was 0.5 sec, which was followed by a beam-off rf time of 50 msec for spin manipulation. After the rf time, a β-ray counting time with the beam off was 1.8 sec. The ^{8}B nuclei ejected at 13° relative to the incident beam direction were caught in a catcher. We obtained a typical β-ray counting rate of about 3×10^{2}/sec with a beam intensity of about 15 μA and a polarization of about 6% [5]. For the measurement of the β-decay asymmetry, β rays were detected by two sets of plastic-scintillator-counter telescopes placed along the static magnetic field (H_0) axis such that one was above (0) and the other below (π) the catcher. Energy discrimination further ensured that only β particles from ^{8}B caught in the catcher were counted. We observed the change of β-ray asymmetry defined by

$$\Delta = [\{W(0)/W(\pi)\}_{\text{on}}/\{W(0)/W(\pi)\}_{\text{off}} - 1]$$
$$\sim 2A(P_{\text{on}} - P_{\text{off}}),$$

where $W(\Theta)$ is the β-ray angular distribution function and A is the asymmetry parameter. P_{on} and P_{off} are the spin polarizations for the count sections with and without rf, respectively. For the detection of β-NMR, a pair of beam-count cycles, one with rf applied and the other without rf applied were repeated until necessary counting statistics were obtained. With the polarization completely destroyed at the rf-on time, the effect of about $-2AP_{\text{off}}$ was observed. In this way, the NMR effect was independent of the instrumental asymmetry in the detection system, and of the time-dependent fluctuations in the beam intensity.

For a given quadrupole coupling constant $\nu_Q = 3eq \times Q/2I(2I-1)h$ ($=eqQ/4h$ for $I=2$), a set of all $2I=4$ transitions is obtained theoretically if the Larmor frequency ν_L, the asymmetry of the field gradient η, and the orientation angle θ of q relative to H_0 are given. The transition frequency ν_m for an $m \leftrightarrow (m-1)$ transition is given in first-order perturbation theory for the $\eta=0$ case as [6] $\nu_m = \nu_L = \frac{1}{2}\nu_Q(m-\frac{1}{2})(3\cos^2\theta - 1)$. Therefore, ν_m is a simple function of ν_Q if the ν_L, θ, η ($=0$ for the present cases) are available. The Larmor frequency for H_0 is determined by the β-NMR detection of the ^{8}B implanted in Pt metal.

The NNQR detection is a variation of the β-NMR detection; an NMR was detected as a function of ν_Q. In an rf time, the four transition frequencies of a set for a given ν_Q were applied in series and the set was repeated typically 11 times within the rf time. The typical time duration for a transition frequency was 1 msec, and that for a set of four frequencies was 4.1 msec in which 25 μsec was for each change of frequency. Suppose 10 values of ν_Q were mapped in a ν_Q spectrum measurement; 3 rf-off cycles were added for normalization. Then (10+3) beam-count cycles were repeated until sufficient counting statistics were attained. The whole rf-handling system was controlled by a microcomputer; beam handling and on-line data taking were carried out using the computer simultaneously. As a result, with a proper rf intensity the polarization can be destroyed completely at the frequencies that reflect the real ν_Q. Such complete destruction is in vivid contrast to the partial destruction detected for a single line only which is about $\frac{1}{20}$ of the maximum effect by the old β-NMR.

The NNQR was detected as a function of θ. In the Mg(hcp) crystal, the ^{8}B and ^{12}B nuclei were mainly located in an interstitial site [4]. In that site the field gradient was symmetric, $\eta=0$, and was parallel to the crystal c axis. The details of the hyperfine interactions of the nuclides in the catchers will be published elsewhere. On the contrary, the final sites of the B isotopes in BN(hcp) [7] were substitutional, and the implanted ^{12}B received the same field gradient as that of the stable isotope ^{11}B. A typical NNQR spectrum of ^{8}B ($I^\pi = 2^+$) implanted in an interstitial site of single crystal Mg is given in Fig. 1. The solid curve in the figure is the theoretical best fit to the data. In the calculation, besides the four transitions ν_m, a dipolar broadening, a spread in the field gradient $\Delta q/q$, rf intensities, and double quantum transitions (DQ) were taken into account. $\Delta q/q \sim 5\%$ was obtained. The small peak at the coupling frequency of $\frac{1}{3}$ of that for the main peak is because the inner two transitions were induced by the outer two rf's among the four that corresponded to the lower coupling frequency. Because of the small transition probabilities for the DQ its peak is hidden in between the two peaks. Experimental results are given in Table I. The ratio $|Q(^{12}\text{B})/Q(^{11}\text{B})| = 0.325 \pm 0.006$ was calculated using the results of ^{12}B and ^{11}B in BN at room temperature, $|eqQ(^{12}\text{B;BN})/h| = 944 \pm 17$ kHz, and $|eqQ(^{11}\text{B;BN})/h| = 2902 \pm 12$ kHz, which was measured by use of the Fourier-transformed NMR (FT-NMR) at high field and was $(1.4 \pm 0.6)\%$ smaller than the value at 4 K [8]. Adopting $Q(^{11}\text{B}, \frac{3}{2}^-) = +40.65 \pm 0.26$ mb [9], $|Q(^{12}\text{B}, 1^+)| = 13.21 \pm 0.26$ mb was determined, in perfect agreement with the known value [3]. For ^{8}B, the ratio of $|Q(^8\text{B})/Q(^{12}\text{B})| = 5.18 \pm 0.13$ was determined from the $|eqQ(^8\text{B;Mg})/h| = 243.6 \pm 6.0$ kHz, and $|eqQ(^{12}\text{B;Mg})/h| = 47.0 \pm 0.1$ kHz which were measured at room temperature. Finally, the quadrupole moment $|Q(^8\text{B}, 2^+)| = 68.3 \pm 2.1$ mb was determined.

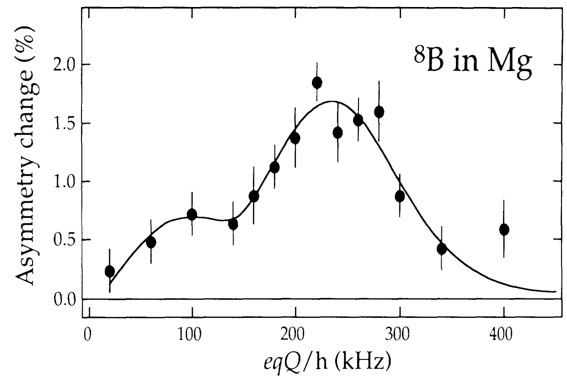

FIG. 1. Typical NNQR of ^{8}B in Mg as a function of the coupling frequency. The solid curve is the theoretical best fit to the data. In the calculation, a dipolar broadening, a spread in the field gradient, rf intensities, and double quantum transitions were taken into account. The smaller peak at the lower coupling frequency than that of the main peak was because the inner two transitions were induced by the outer two rf's among the four rf's that corresponded to the lower coupling frequency; the polarization was only partially destroyed. A possible peak that corresponds to the DQ, that lies in between the two peaks, is hidden because of the low transition probabilities.

TABLE I. The measured quadrupole moments $Q(^8\mathrm{B},2^+)$, $Q(^8\mathrm{Li},2^+)$, and $Q(^{12}\mathrm{B},1^+)$.

$A(I^\pi)$	Catcher (T)	Site	$\lvert eqQ/h \rvert$ (kHz)	Reference
$^{11}\mathrm{B}(\frac{3}{2}^-)$	BN (~300 K)	Substitutional	2902 ± 12	Present [a]
$^{12}\mathrm{B}(1^+)$	BN (~300 K)	Substitutional	944 ± 17	Present
$^{12}\mathrm{B}(1^+)$	Mg (~300 K)	Interstitial	47.0 ± 0.1	Present
$^{8}\mathrm{B}(2^+)$	Mg (~300 K)	Interstitial	243.6 ± 6.0	Present
		$\lvert Q(^{12}\mathrm{B},1^+)\rvert = 13.21 \pm 0.26$ mb		Present [b]
		$\lvert Q(^{8}\mathrm{B},2^+)\rvert = 68.3 \pm 2.1$ mb		Present
$^{8}\mathrm{Li}(2^+)$	$\mathrm{LiIO_3}$ (~300 K)		29.24 ± 0.36	Present
			29.2 ± 0.8	[10]
	$\mathrm{LiNbO_3}$ (~300 K)		44.68 ± 0.88	Present
			43 ± 3	[11]
$^{7}\mathrm{Li}(\frac{3}{2}^-)$	$\mathrm{LiIO_3}$ (~300 K)		36.4 ± 0.5	Present
			44 ± 3	[13]
	$\mathrm{LiNbO_3}$ (~300 K)		53.3 ± 1.1	Present
			54.5 ± 0.5	[11]
		$\lvert Q(^{8}\mathrm{Li};\mathrm{LiIO_3})\rvert = 32.1 \pm 0.8$ mb		Present
		$\lvert Q(^{8}\mathrm{Li};\mathrm{LiNbO_3})\rvert = 33.5 \pm 1.1$ mb		Present
Averaged		$\lvert Q(^{8}\mathrm{Li};2^+)\rvert = 32.7 \pm 0.6$ mb		Present

[a] At 4 K $\lvert eqQ/h\rvert = 2943 \pm 4$ kHz (Ref. [8]).
[b] $Q(^{12}\mathrm{B},1^+) = 13.4 \pm 1.4$ mb (Ref. [3]).

A long-standing open question [10,11] about the $Q(^8\mathrm{Li},2^+)$ value of ^{8}Li has been decisively ended by the present NNQR detections of ^{8}Li and FT-NMR detections of ^{7}Li in $\mathrm{LiIO_3}$ and $\mathrm{LiNbO_3}$ crystals. The coupling constants of ^{8}Li in the substitutional sites of single crystals of $\mathrm{LiIO_3}$ and $\mathrm{LiNbO_3}$ were determined as $\lvert eqQ(^8\mathrm{Li};\mathrm{LiIO_3})/h\rvert = 29.24 \pm 0.36$ kHz and $\lvert eqQ(^8\mathrm{Li};\mathrm{LiNbO_3})/h\rvert = 44.68 \pm 0.88$ kHz, respectively. These values are in quite good agreement with the known values. The field gradients in the substitutional sites of both crystals were also remeasured by detecting FT-NMR at high field, $\lvert eqQ(^7\mathrm{Li};\mathrm{LiIO_3})/h\rvert = 36.4 \pm 0.5$ kHz and $\lvert eqQ(^7\mathrm{Li};\mathrm{LiNbO_3})/h\rvert = 53.3 \pm 1.1$ kHz for both crystals. Adopting the recent result of $Q(^7\mathrm{Li}) = -40.0 \pm 0.6$ mb [12], $Q(^8\mathrm{Li},2^+)$ values from both catchers were determined as $\lvert Q(^8\mathrm{Li},2^+)\rvert = 32.1 \pm 0.8$ mb, and 33.5 ± 1.1 mb as shown in Table I. Finally, from the average of the two, $\lvert Q(^8\mathrm{Li},2^+)\rvert = 32.7 \pm 0.6$ mb was determined. Experimental details of the present hyperfine interaction studies of ^{7,8}Li isotopes will be reported elsewhere.

The nuclear quadrupole moment of a state is separated into two matrix elements $\tilde{Q}(N_p)$ and $\tilde{Q}(N_n)$ by the proton-neutron formalism

$$Q(N_p,N_n) = \left(\frac{16\pi}{5}\right)^{1/2} \left[\left\langle \sum e_n^{\mathrm{eff}}(\tfrac{1}{2}+t_z) r_i^2 Y_{20}(\Omega_i)\right\rangle + \left\langle \sum e_p^{\mathrm{eff}}(\tfrac{1}{2}-t_z) r_i^2 Y_{20}(\Omega_i)\right\rangle\right] = e_n^{\mathrm{eff}}\tilde{Q}(N_n) + e_p^{\mathrm{eff}}\tilde{Q}(N_p),$$

where t_z is the z component of the isospin operator. The effective charges of the proton and the neutron in light nuclei are obtained by Sagawa and Brown [14] as $e_p^{\mathrm{eff}} = +1.3e$ and $e_n^{\mathrm{eff}} = +0.5e$. The density distributions of protons and neutrons in ^{8}B as a function of radius are calculated by use of the Cohen-Kurath (CK) shell-model wave functions in the Woods-Saxon (WS) potential, as shown in Fig. 2. The parameters of the Woods-Saxon potential are taken from Ref. [15] except for the potential depth. The depth is adjusted to reproduce the experimental separation energy of the single-particle state in each shell-model configuration [16]. The solid curve for the proton distribution shows a substantial radial swelling overcoming the Coulomb and centrifugal barriers compared with the distribution of neutrons shown by the dashed curve. Since the densities close to the surface are mainly due to the valence nucleons as shown by the dotted curves, the value $\tilde{Q}_{\mathrm{th}}(N)$ reflects the distribution of the valence nucleons. The shell-model calculation is reliable in predicting the $\tilde{Q}_{\mathrm{th}}(N)$ for the deeply bound nucleons, and gives the same value of $\tilde{Q}_{\mathrm{th}}(3) = 8.5$ mb for both the three-neutron configuration in ^{8}B and the three-proton configuration in ^{8}Li. Therefore we are able to extract the value for five protons in the ^{8}B nucleus semiempirically as

$$\tilde{Q}_{\mathrm{expt}}(5) = [Q_{\mathrm{expt}}(^8\mathrm{B},2^+) - e_n^{\mathrm{eff}}\tilde{Q}_{\mathrm{th}}(3)]/e_p^{\mathrm{eff}}$$
$$= [68.3 - 0.5\times 8.5]/1.3 = 49.3\ \mathrm{mb}.$$

If the five protons were deeply bound, the theory predicts

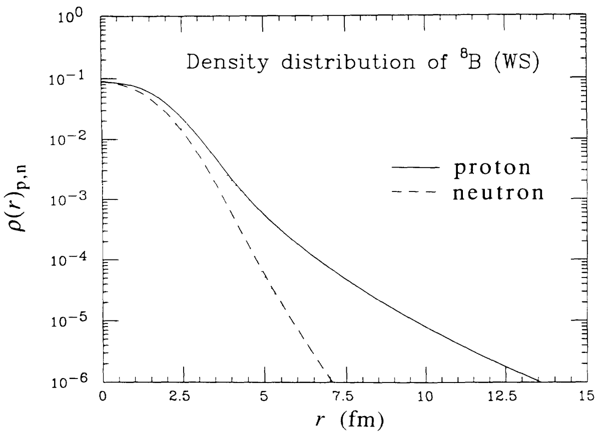

FIG. 2. Density distributions in ^{8}B. The densities were obtained by using the spectroscopic factors of the Cohen-Kurath shell-model calculations, and the single-particle wave functions in the Woods-Saxon potential. The depth of the potential is adjusted to reproduce the separation energy of the shell-model configuration. The solid and broken curves correspond to proton and neutron distributions, respectively. The dotted lines are those for valence nucleons.

$\tilde{Q}_{th}(5)$(WS;deep) $=24.3$ mb, which is about half of the empirical value. Taking into account the proton separation energy, i.e., the halo effect in ^{8}B, we obtain $\tilde{Q}_{th}(5)$(WS) $=49.5$ mb which agrees perfectly with the empirical value. The rms radius $\langle r^2\rangle^{1/2}=2.98$ fm calculated with the halo effect for the protons is larger than $\langle r^2\rangle^{1/2}=2.20$ fm for the three-neutron core. This is clear evidence for a proton halo covering ^{7}Be in ^{8}B. For a complete discussion with the present recipe, we also study the mirror partner ^{8}Li where the proton and neutron are both deeply bound (12.5 and 2.0 MeV, respectively). The theoretical value for five neutrons $\tilde{Q}_{th}(5)=39.4$ mb gives the quadrupole moment $Q_{th}(^8\mathrm{Li},2^+)=30.5$ mb which accounts completely for the experimental value $|Q_{expt}(^8\mathrm{Li},2^+)|=32.7\pm0.6$ mb. The value $\tilde{Q}_{th}(5)$ in ^{8}Li suggests a thin neutron skin covering the ^{7}Li core. The present rms radius for protons in ^{8}B is about 20% larger than the value of $\langle r^2\rangle^{1/2}=2.45$ fm determined from the interaction cross sections [1], which corresponds to about a 30% difference in the interaction cross section, using a radioactive beam of 800-MeV/nucleon ^{8}B. On the other hand, radii determined by two methods agree well with each other for neutrons. The large difference between radii for protons determined by two methods is not well understood presently. Detailed theoretical studies of the origin of the discrepancy are necessary as well as experimental ones.

In conclusion, we measured the quadrupole moment of ^{8}B as $|Q(^8\mathrm{B},2^+)|=68.3\pm2.1$ mb by use of the modified β-NMR. The value was accounted for fairly well by the effect of the spatial swelling of the proton distribution. A prominent proton halo is suggested covering the ^{7}Be core in spite of the existence of the Coulomb and centrifugal barriers in ^{8}B.

We thank G. Krebs, LBL, for his suggestions and a careful reading of the present manuscript. The present work was partially supported by the Grant in Aid for Scientific Research and Monbusho International Scientific Program given by the Ministry of Education, Culture and Science. Support was also given by the U.S.A.-Japan Collaborative Research, given by both the Japan Scientific Foundation, and the National Science Foundation, U.S.A. This work was also partially supported by the Yamada Science Foundation. The numerical calculations were done at the VAX 6000-440 computer at The Meson Science Research Center, University of Tokyo, and the VAX VS-3100/GPX at RCNP, Osaka University.

[a] Present address: National Institute of Radiological Sciences, 4-9-1 Anagawa, Inage-ku, Chiba 263, Japan.

[1] I. Tanihata *et al.*, Phys. Rev. Lett. **55**, 2676 (1985); Nucl. Phys. **A520**, 411C (1990); Phys. Lett. **206**, 592 (1988).
[2] T. Minamisono, J. Phys. Soc. Jpn. Suppl. **34**, 324 (1973).
[3] T. Minamisono, S. Kogo, K. Okajima, and K. Sugimoto, Hyperfine Interact. **4**, 224 (1978).
[4] A. Kitagawa, K. Matsuta, Y. Nojiri, and T. Minamisono, Hyperfine Interact. **60**, 869 (1990).
[5] T. Minamisono, Y. Nojiri, A. Mizobuchi, and K. Sugimoto, J. Phys. Soc. Jpn. Suppl. **34**, 156 (1973).
[6] A. Abragam, *The Principles of Nuclear Magnetism* (Clarendon, Oxford, England, 1961).
[7] Provided from Denka Research Center, 3-5-1 Asahimachi, Machida, Tokyo 194, Japan.
[8] C. Connor *et al.*, Rev. Sci. Instrum. **61**, 1059 (1990).
[9] R. K. Nesbet, Phys. Rev. A **2**, 1208 (1970); D. Sundholm and J. Olsen, J. Chem. Phys. **94**, 5051 (1991).
[10] T. Minamisono, J. W. Hugg, D. G. Mavis, T. K. Saylor, S. M. Lazarus, H. F. Glavish, and S. S. Hanna, Phys. Rev. Lett. **34**, 1465 (1975).
[11] H. Ackermann *et al.*, Phys. Lett. **52B**, 54 (1974).
[12] M. Urban and A. J. Sandlej, Chem. Phys. Lett. **173**, 157 (1990); H.-G. Voelk and D. Fick, Nucl. Phys. **A530**, 475 (1991).
[13] V. M. Sarnatskii, V. A. Shutilov, T. D. Levitskaya, B. I. Kidyarov, and P. L. Mitnitskii, Fiz. Tverd. Tela (Leningrad) **13**, 2413 (1971) [Sov. Phys. Solid State **13**, 2021 (1972)].
[14] H. Sagawa and B. A. Brown, Nucl. Phys. **A430**, 84 (1984).
[15] A. Bohr and B. R. Mottelson, *Nuclear Structure* (Benjamin, Menlo Park, 1969), Vol. 1, p. 239.
[16] H. Kitagawa and H. Sagawa, Nucl. Phys. A (to be published).